Supplement of Hydrol. Earth Syst. Sci., 30, 289–315, 2026
https://doi.org/10.5194/hess-30-289-2026-supplement

Hydrology and Earth System Sciences
Open Access

Supplement of

High resolution monthly precipitation isotope estimates across Australia from machine learning

Georgina Falster et al.

Correspondence to: Georgina Falster (georgina.falster@adelaide.edu.au)

Table S1: Details for each site contributing water isotope observations to this study. Sites are arranged by latitude, northernmost to southernmost. An entry of 'some' in the 'Publicly available' column indicates that some but not all of the data from that site was publicly available at the time of this manuscript's publication. Note that for most GNIP sites, data through to the end of 2014 is described in Hollins et al., 2018 then data from 2015 to 2023 is described in Hughes et al., 2025. An entry of 'pers. comm.' in the 'Publicly available' column indicates that currently unpublished data were provided directly to the first author. GNIP = Global Network of Isotopes in Precipitation; CSIRO = Commonwealth Scientific and Industrial Research Organisation.

Site name	**Latitude**	**Longitude**	**Elevation (m)**	**Start year**	**End year**	**Total months**	**Total years**	**Original resolution**	**Source/s**	**Publicly available**	**Reference/s**	**Variables measured**
Darwin	-12.4	130.9	30.4	1962	2023	408	55	Daily, Monthly	GNIP, CSIRO, pers. comm.	Some	Crosbie et al., 2012; Duvert et al., 2020; Hollins et al., 2018; Hughes et al., 2025; Munksgaard et al., 2019; Zwart et al., 2018	δ^2H, $\delta^{18}O$
Willis Island	-16.3	150	9.3	2015	2023	86	9	Daily	Pers. comm.	Some	NA	δ^2H, $\delta^{18}O$
Cairns	-16.9	145.8	13.4	2014	2023	114	10	Daily	Pers. comm.	Some	Munksgaard et al., 2019, 2020	δ^2H, $\delta^{18}O$
Chillagoe	-17.2	144.5	368.9	2015	2023	64	9	Daily	Pers. comm.	No	NA	δ^2H, $\delta^{18}O$
Broome	-18	122.2	15	2007	2008	4	2	Monthly	Geoscience Australia	Yes	Hawkins et al., 2022	δ^2H, $\delta^{18}O$
Halls Creek	-18.2	127.7	408.1	2008	2010	15	3	Monthly	CSIRO	Yes	Crosbie et al., 2012	δ^2H, $\delta^{18}O$
Tennant Creek	-19.6	134.2	373.3	2007	2008	6	2	Monthly	Geoscience Australia	Yes	Hawkins et al., 2022	δ^2H, $\delta^{18}O$
Mount Isa	-20.7	139.5	340.3	2006	2023	111	18	Monthly	GNIP, CSIRO	Yes	Crosbie et al., 2012; Hollins et al., 2018; Hughes et al., 2025	δ^2H, $\delta^{18}O$
Exmouth	-21.9	114.1	11.8	2008	2009	2	2	Monthly	CSIRO	Yes	Crosbie et al., 2012	δ^2H, $\delta^{18}O$
Rockhampton	-23.4	150.5	2.8	2008	2010	17	3	Monthly	CSIRO	Yes	Crosbie et al., 2012	δ^2H, $\delta^{18}O$
Alice Springs	-23.8	133.9	546	1962	2023	273	39	Monthly	GNIP, CSIRO	Yes	Crosbie et al., 2012; Hollins et al., 2018; Hughes et al., 2025	δ^2H, $\delta^{18}O$
Giles	-25	128.3	587.7	2007	2008	9	2	Monthly	Geoscience Australia	Yes	Hawkins et al., 2022	δ^2H, $\delta^{18}O$
Barakula	-26.4	150.5	334	2007	2008	13	2	Monthly	Geoscience Australia	Yes	Hawkins et al., 2022	δ^2H, $\delta^{18}O$

Charleville	-26.4	146.3	301.6	2006	2023	124	18	Monthly	GNIP, CSIRO	Yes	Crosbie et al., 2012; Hollins et al., 2018; Hughes et al., 2025	δ^2H, $\delta^{18}O$
Meekatharra	-26.6	118.5	517	2006	2017	104	12	Monthly	GNIP, CSIRO	Yes	Crosbie et al., 2012; Hollins et al., 2018; Hughes et al., 2025	δ^2H, $\delta^{18}O$
Brisbane	-27.4	153.1	4	1962	2023	573	56	Monthly	GNIP, CSIRO	Yes	Crosbie et al., 2012; Hollins et al., 2018; Hughes et al., 2025	δ^2H, $\delta^{18}O$
Toowoomba	-27.6	152	589.9	2007	2010	20	4	Monthly	CSIRO, Geoscience Australia	Yes	Crosbie et al., 2012; Hawkins et al., 2022	δ^2H, $\delta^{18}O$
Goondiwindi	-28.5	150.3	212.2	2007	2008	6	2	Monthly	Geoscience Australia	Yes	Hawkins et al., 2022	δ^2H, $\delta^{18}O$
Moree	-29.5	149.8	200.3	2007	2008	8	2	Monthly	Geoscience Australia	Yes	Hawkins et al., 2022	δ^2H, $\delta^{18}O$
Warialda	-29.5	150.6	335.5	2007	2008	5	2	Monthly	Geoscience Australia	Yes	Hawkins et al., 2022	δ^2H, $\delta^{18}O$
Narrabri	-30.3	149.8	211.5	2007	2008	4	2	Monthly	Geoscience Australia	Yes	Hawkins et al., 2022	δ^2H, $\delta^{18}O$
Macquarie Marshes	-30.9	147.5	146.6	2008	2014	72	7	Daily	Publication	Yes	Crawford et al., 2017	δ^2H, $\delta^{18}O$
Woomera	-31.2	136.8	166.6	2006	2021	80	15	Monthly	GNIP, CSIRO	Yes	Crosbie et al., 2012; Hollins et al., 2018; Hughes et al., 2025	δ^2H, $\delta^{18}O$
Cobar	-31.5	145.8	260	2006	2016	108	11	Monthly	GNIP, CSIRO	Yes	Crosbie et al., 2012; Hollins et al., 2018; Hughes et al., 2025	δ^2H, $\delta^{18}O$
Nyngan	-31.6	147.2	167.9	2007	2008	5	2	Monthly	Geoscience Australia	Yes	Hawkins et al., 2022	δ^2H, $\delta^{18}O$
Gilgandra	-31.7	148.7	274.5	2007	2008	5	2	Monthly	Geoscience Australia	Yes	Hawkins et al., 2022	δ^2H, $\delta^{18}O$
Perth	-31.9	115.9	15.4	1962	2023	449	47	Monthly	GNIP, CSIRO	Yes	Crosbie et al., 2012; Hollins et al., 2018; Hughes et al., 2025	δ^2H, $\delta^{18}O$
Dubbo	-32.2	148.6	270.8	2007	2008	5	2	Monthly	Geoscience Australia	Yes	Hawkins et al., 2022	δ^2H, $\delta^{18}O$
Wellington	-32.6	148.9	305.1	2011	2013	22	3	Monthly	Publication	Yes	Cuthbert et al., 2014	δ^2H, $\delta^{18}O$

Condobolin	-33.1	147.1	190	2007	2008	4	2	Monthly	Geoscience Australia	Yes	Hawkins et al., 2022	δ^2H, $\delta^{18}O$
Lithgow	-33.5	150.2	957.4	2005	2008	43	4	Monthly	Publication	Yes	Hughes and Crawford, 2013	δ^2H, $\delta^{18}O$
Cowra	-33.8	148.7	319.5	2007	2008	7	2	Monthly	Geoscience Australia	Yes	Hawkins et al., 2022	δ^2H, $\delta^{18}O$
Esperance	-33.9	121.9	7.3	2008	2010	19	3	Monthly	CSIRO	Yes	Crosbie et al., 2012	δ^2H, $\delta^{18}O$
Sydney	-33.9	151.2	6	2006	2023	191	18	Monthly	GNIP, CSIRO	Yes	Crosbie et al., 2012; Hollins et al., 2018; Hughes et al., 2025	δ^2H, $\delta^{18}O$
Calgardup Caves	-34	115	70	2005	2019	150	15	Daily	GNIP	Yes	Griffiths et al., 2022	δ^2H, $\delta^{18}O$
Lucas Heights	-34.1	151	99.3	2005	2020	149	15	Daily, Monthly	Publication	Some	Crawford et al., 2023; Hughes and Crawford, 2013	δ^2H, $\delta^{18}O$
Mount Werong	-34.1	149.9	1119.5	2005	2009	54	5	Monthly	Publication	Yes	Hughes and Crawford, 2013	δ^2H, $\delta^{18}O$
Taylorville	-34.1	139.9	15.6	2007	2007	3	1	Monthly	Geoscience Australia	Yes	Hawkins et al., 2022	δ^2H, $\delta^{18}O$
Mildura	-34.2	142.1	50	2006	2014	94	9	Monthly	GNIP, CSIRO	Yes	Crosbie et al., 2012; Hollins et al., 2018; Hughes et al., 2025	δ^2H, $\delta^{18}O$
Loxton	-34.5	140.6	28.8	2007	2007	3	1	Monthly	Geoscience Australia	Yes	Hawkins et al., 2022	δ^2H, $\delta^{18}O$
Big Hill	-34.6	150	656.8	2005	2008	35	4	Monthly	Publication	Yes	Hughes and Crawford, 2013	δ^2H, $\delta^{18}O$
Adelaide	-34.9	138.6	34.1	1962	2023	317	32	Monthly	GNIP, CSIRO	Yes	Crosbie et al., 2012; Hollins et al., 2018; Hughes et al., 2025	δ^2H, $\delta^{18}O$
Murray Bridge	-35.1	139.3	13.7	2007	2008	8	2	Monthly	Geoscience Australia	Yes	Hawkins et al., 2022	δ^2H, $\delta^{18}O$
Evatt	-35.2	149.1	598.5	2007	2008	12	2	Monthly	Geoscience Australia	Yes	Hawkins et al., 2022	δ^2H, $\delta^{18}O$
Wagga Wagga	-35.2	147.5	212	2006	2021	169	16	Monthly	GNIP, CSIRO	Yes	Crosbie et al., 2012; Hollins et al., 2018; Hughes et al., 2025	δ^2H, $\delta^{18}O$
Tarcutta	-35.3	147.7	226.5	2007	2008	7	2	Monthly	Geoscience Australia	Yes	Hawkins et al., 2022	δ^2H, $\delta^{18}O$

Braidwood	-35.4	149.8	644	2006	2008	21	3	Monthly	Geoscience Australia	Yes	Hawkins et al., 2022	δ^2H, $\delta^{18}O$
Googong	-35.4	149.2	721.9	2007	2008	12	2	Monthly	Geoscience Australia	Yes	Hawkins et al., 2022	δ^2H, $\delta^{18}O$
Tidbinbilla	-35.4	148.9	1121	2007	2008	14	2	Monthly	Geoscience Australia	Yes	Hawkins et al., 2022	δ^2H, $\delta^{18}O$
Wilkawatt	-35.4	140.4	93.3	2007	2008	2	2	Monthly	Geoscience Australia	Yes	Hawkins et al., 2022	δ^2H, $\delta^{18}O$
Deniliquin	-35.5	144.9	91.7	2007	2008	5	2	Monthly	Geoscience Australia	Yes	Hawkins et al., 2022	δ^2H, $\delta^{18}O$
Yarrangobilly	-35.7	148.5	1098.2	2007	2017	112	11	Monthly	Publication	No	NA (not currently available from publication)	δ^2H, $\delta^{18}O$
Kelly Hill	-36	136.9	28.7	2011	2013	24	3	Daily	Pers. comm.	No	NA	δ^2H, $\delta^{18}O$
Albury	-36.1	146.9	196.3	2007	2008	6	2	Monthly	Geoscience Australia	Yes	Hawkins et al., 2022	δ^2H, $\delta^{18}O$
Horsham	-36.7	142.2	127.2	2007	2008	11	2	Monthly	Geoscience Australia	Yes	Hawkins et al., 2022	δ^2H, $\delta^{18}O$
Learmonth	-37.4	143.7	434.3	2008	2010	9	3	Monthly	CSIRO	Yes	Crosbie et al., 2012	δ^2H, $\delta^{18}O$
Melbourne	-37.8	145	113	1962	2023	536	52	Monthly	GNIP, CSIRO	Yes	Crosbie et al., 2012; Hollins et al., 2018; Hughes et al., 2025	δ^2H, $\delta^{18}O$
Cape Grim	-40.7	144.7	94	1979	2023	433	42	Monthly	GNIP, CSIRO	Yes	Crosbie et al., 2012; Hollins et al., 2018; Hughes et al., 2025	δ^2H, $\delta^{18}O$
Hobart	-42.8	147.5	8.8	2019	2022	37	4	Daily	Unpublished (from the lead author)	No	NA	δ^2H, $\delta^{18}O$
Margate	-43	147.3	120.9	1994	2000	18	7	Monthly	GNIP	Yes	Hollins et al., 2018	$\delta^{18}O$

Table S2: Details of predictor variables included in the random forest models. The first column shows the variable name as it appears in figures throughout the manuscript. Variables flagged as 'direct' are used without modification from the original source (e.g., ERA5) other than regridding where required. Where relevant, the 'Source' column entry is a reference containing the details of how the predictor variable was calculated from the raw meteorological data (not included if the variable required only a ratio and/or conversion from native units).

Variable name	Variable long name	Variable name/s in ERA5	Direct or derived	Source
Meteorological variables				
Temp	Air temperature at 2 metres	2t	Direct	NA
Evap	Evaporation	mer	Derived	NA
Snow_frac	Fraction of precipitation delivered as snow	sf,tp	Derived	NA
MSLP	Mean sea level pressure	msl	Direct	NA
Prec	Precipitation amount	tp	Derived	NA
Prec_int	Precipitation intensity	pr	Derived	NA
Prec_type	Ratio of convective to total precipitation	cp,tp	Derived	NA
RH	Relative humidity	2t,2d	Derived	Sonntag, 1990
Wind_dir	Wind direction at 10 metres	10u,10v	Derived	NA
Wind_speed	Wind speed at 10 metres	10si	Direct	NA
Climate indices				
ΔSLP	Trans-Pacific sea level pressure gradient	msl	Derived	Vecchi et al., 2006
DMI	Dipole Mode Index	sst	Derived	Saji et al., 1999
IOBM	Indian Ocean Basin Mode	sst	Derived	Yu et al., 2022
Niño 3.4	Niño 3.4	sst	Derived	See Section 2.3
SAM	Southern Annular Mode	msl	Derived	Velasquez-Jimenez and Abram, 2024
Weather objects				
Anticyclone	Anticyclone	NA	Derived	Jin et al., 2024
COL_trop	Cutoff low (troposphere)	NA	Derived	Jin et al., 2024
COL_strat	Cutoff low (stratosphere)	NA	Derived	Jin et al., 2024
Cyclone	Cyclone	NA	Derived	Jin et al., 2024
Front	Front	NA	Derived	Jin et al., 2024
PV_streamer	Potential vorticity streamer	NA	Derived	Jin et al., 2024
WCB_ascent	Warm conveyor belt (ascent)	NA	Derived	Jin et al., 2024
WCB_inflow	Warm conveyor belt (inflow)	NA	Derived	Jin et al., 2024
Other				
Month_s	Month (sine)	NA	Direct	NA
Month_c	Month (cosine)	NA	Direct	NA
Elev	Elevation	NA	Direct	NA

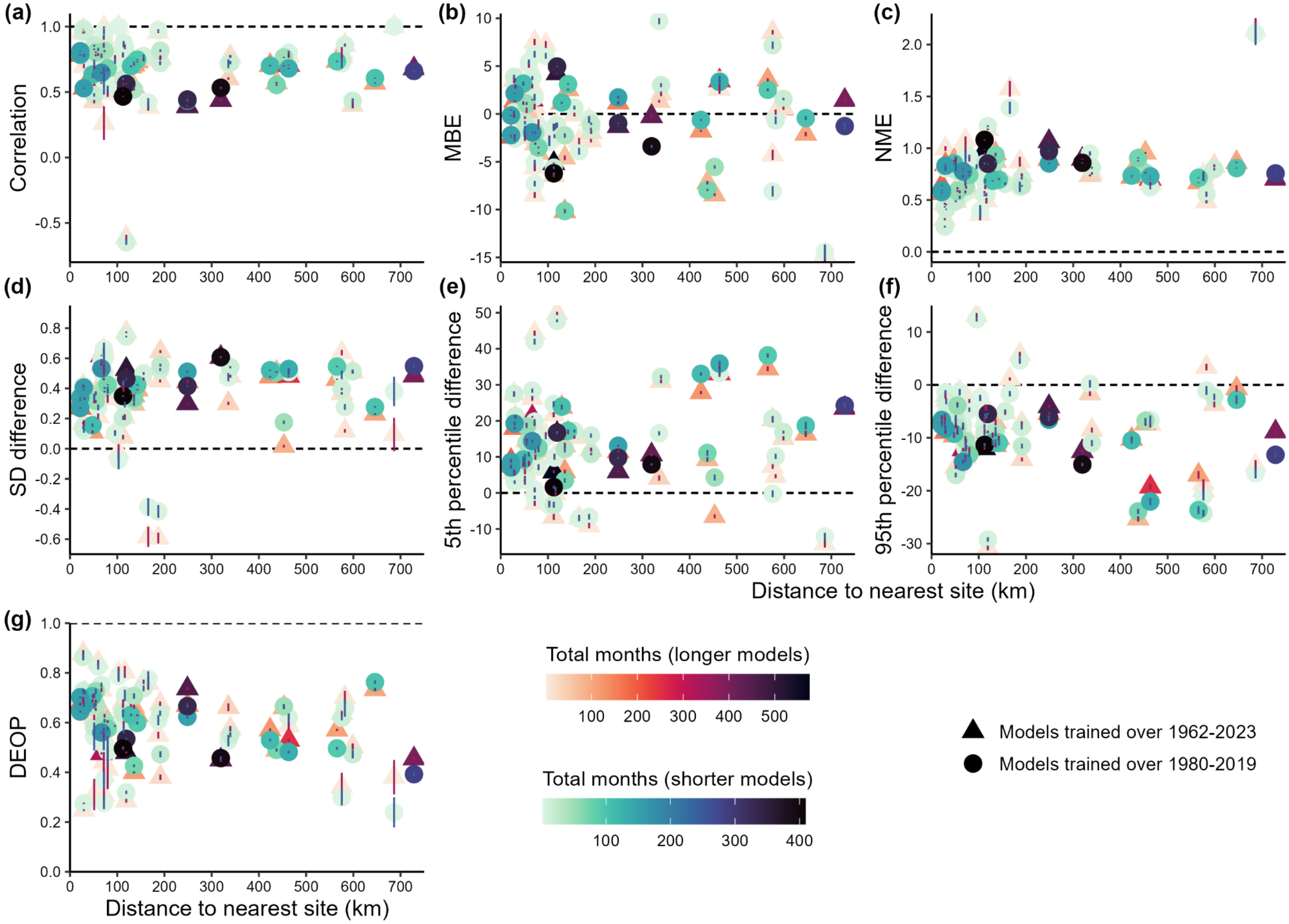

Figure S1: As per Fig. 1 but showing skill scores for out-of-sample spatial δ^2H_P variability.

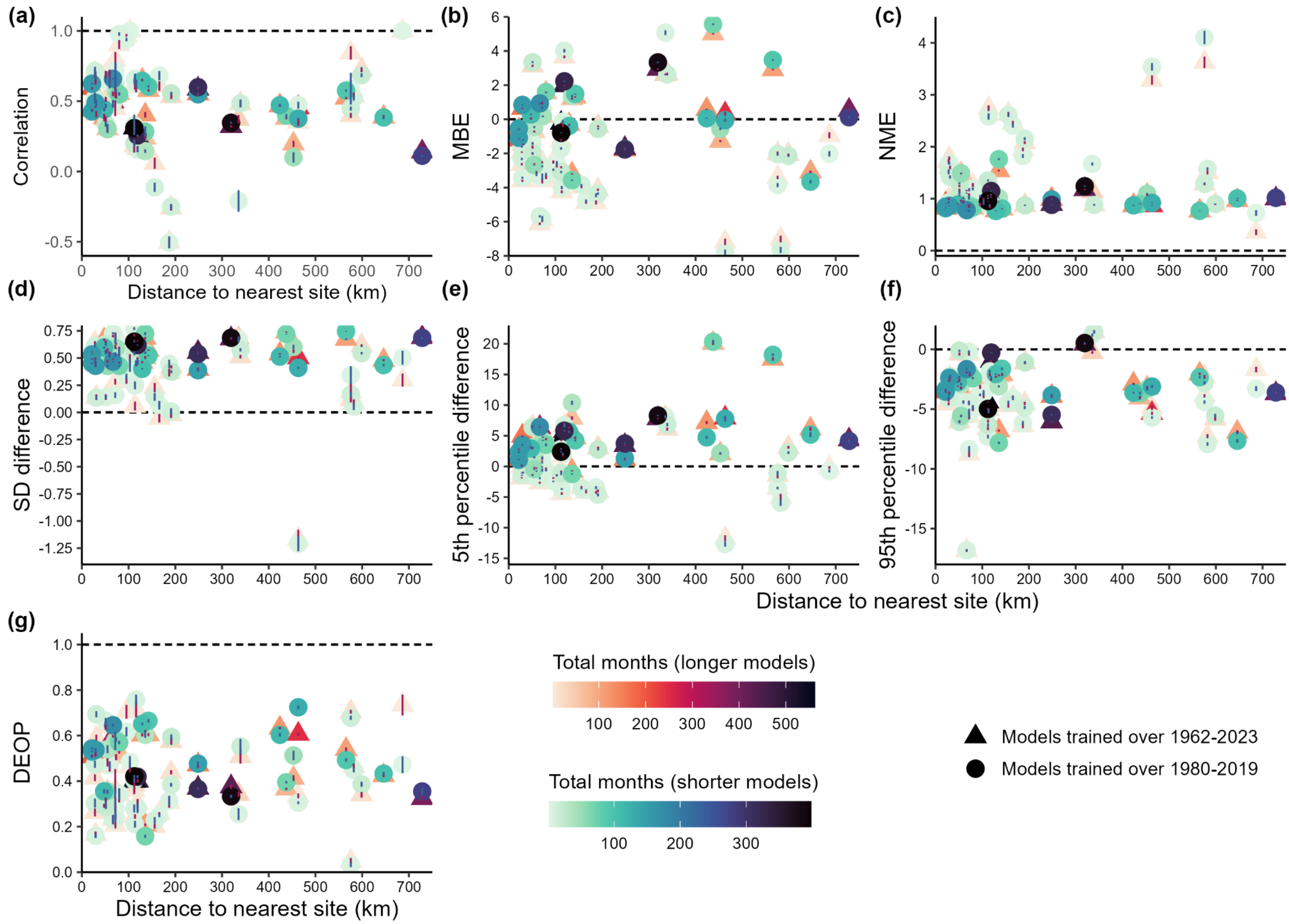

Figure S2: As per Fig. 1 but showing skill scores for out-of-sample spatial dxs_P variability.

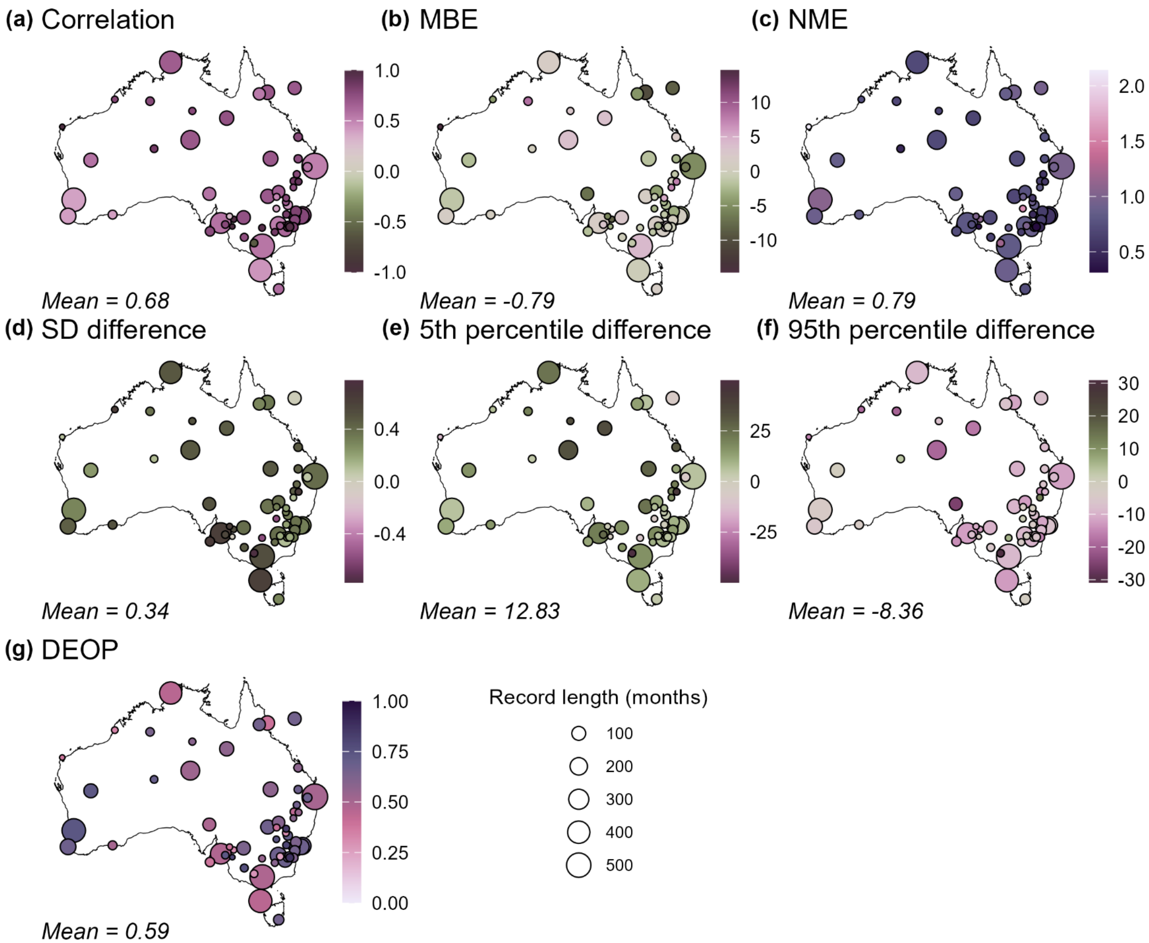

Figure S3: As per Fig. 2 but showing skill scores for out-of-sample spatial δ^2H_P variability.

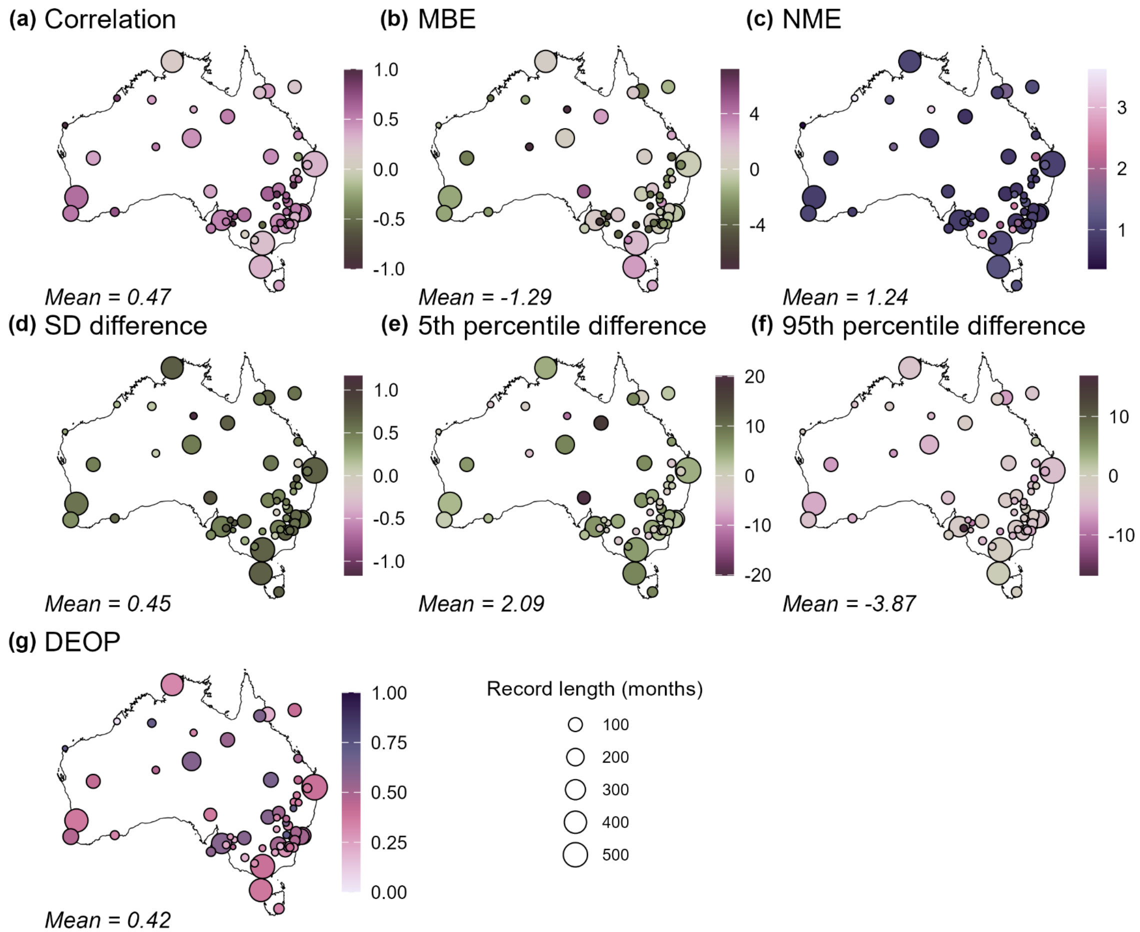

Figure S4: As per Fig. 2 but showing skill scores for out-of-sample spatial dxs_P variability.

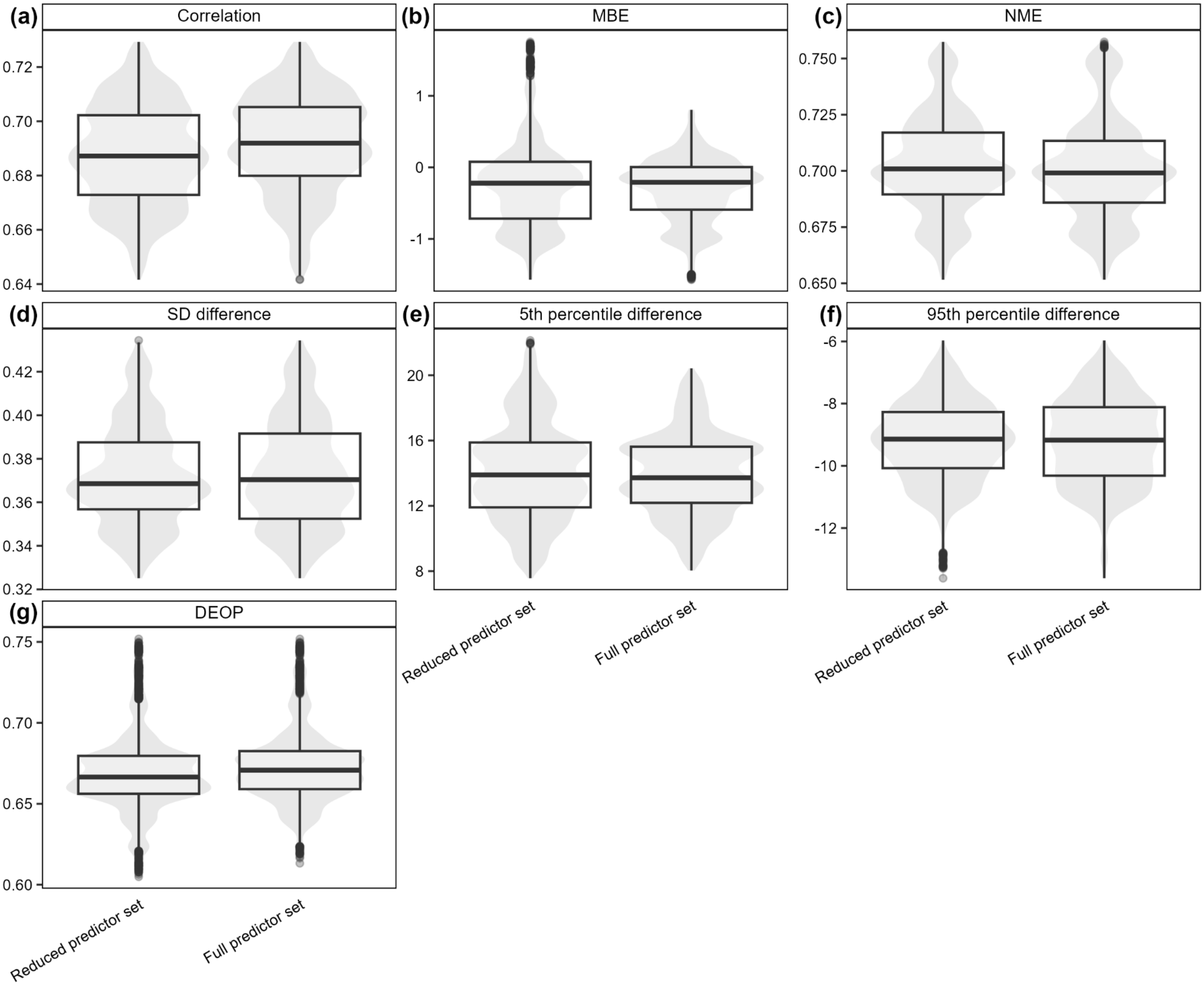

Figure S5: As per Fig. 3 but showing skill scores for out-of-sample temporal δ^2H_P variability.

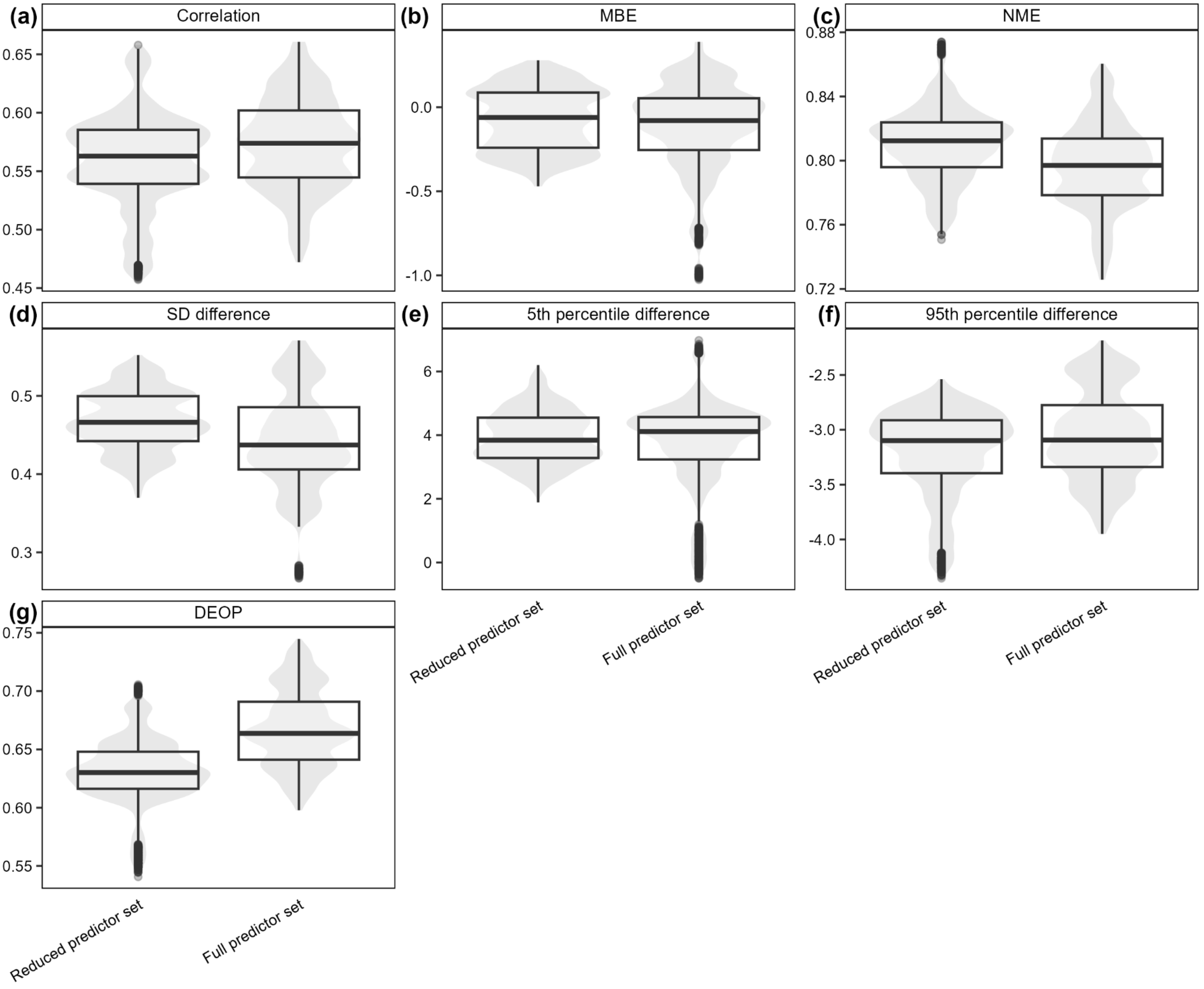

Figure S6: As per Fig. 3 but showing skill scores for out-of-sample temporal dxs_P variability.

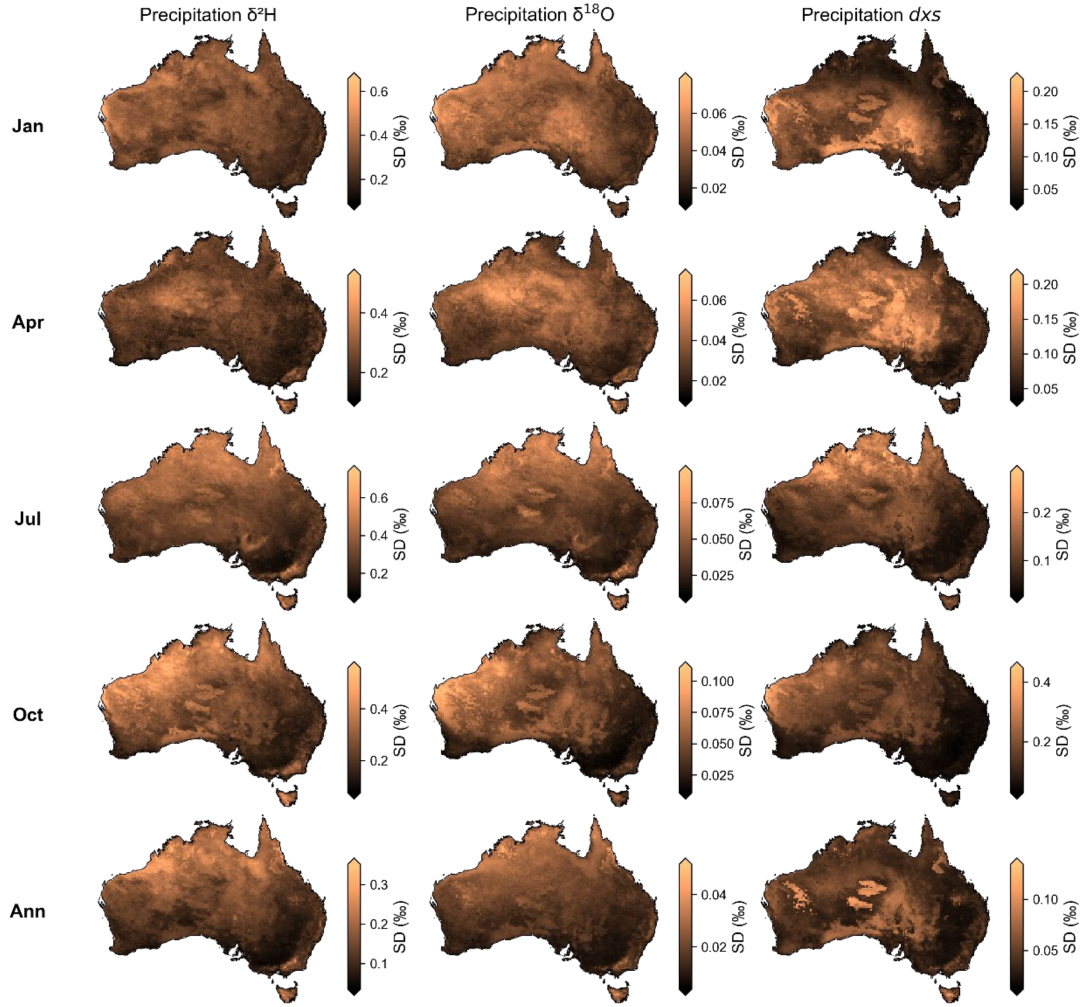

Figure S7: Standard deviation of random forest-modelled monthly (rows one to four) and annual (row five) precipitation isotopic variability, across the 50 random forest model ensemble members. Standard deviations calculated on the long-term monthly mean (rows one to four) or precipitation-weighted annual mean (row five), across the 50 models created with unique random seeds. Here showing only the central month of each season. Ensemble standard deviations calculated using the random forest models trained over 1962–2023, using the reduced set of predictor variables (without weather objects).

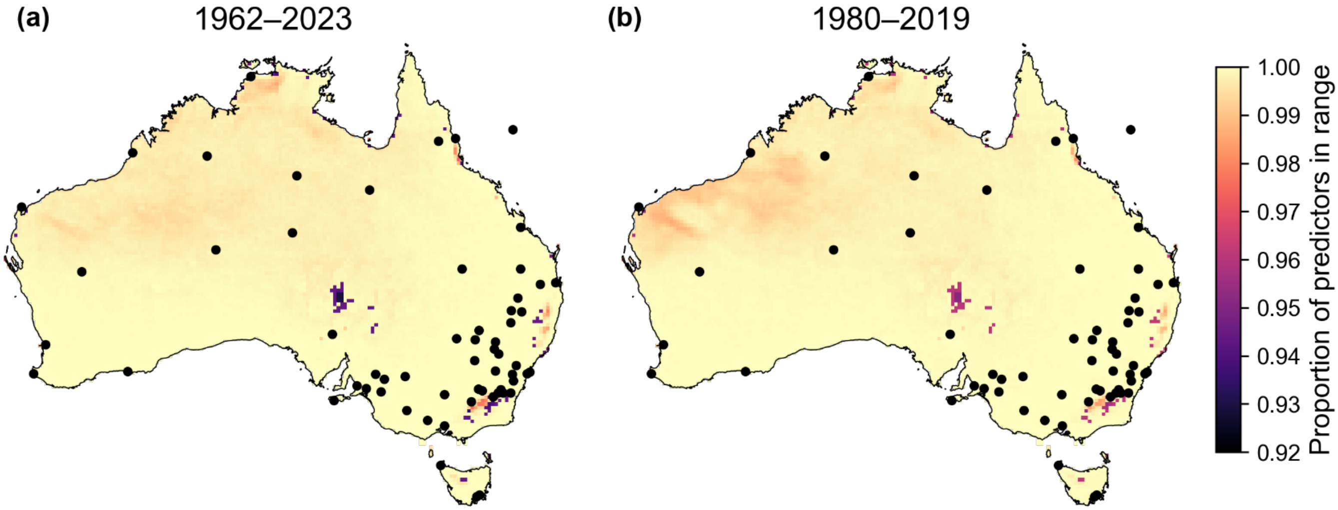

Figure S8: Proportion of predictor variables that are within range of the training dataset. Panel a) shows values for the longer models trained over 1962–2023, using the reduced set of predictor variables (without weather objects). Panel b) shows values for the models trained over 1980–2019, using the full set of predictor variables (including weather objects). Points show locations of sites contributing precipitation isotopic data to the random forest models.

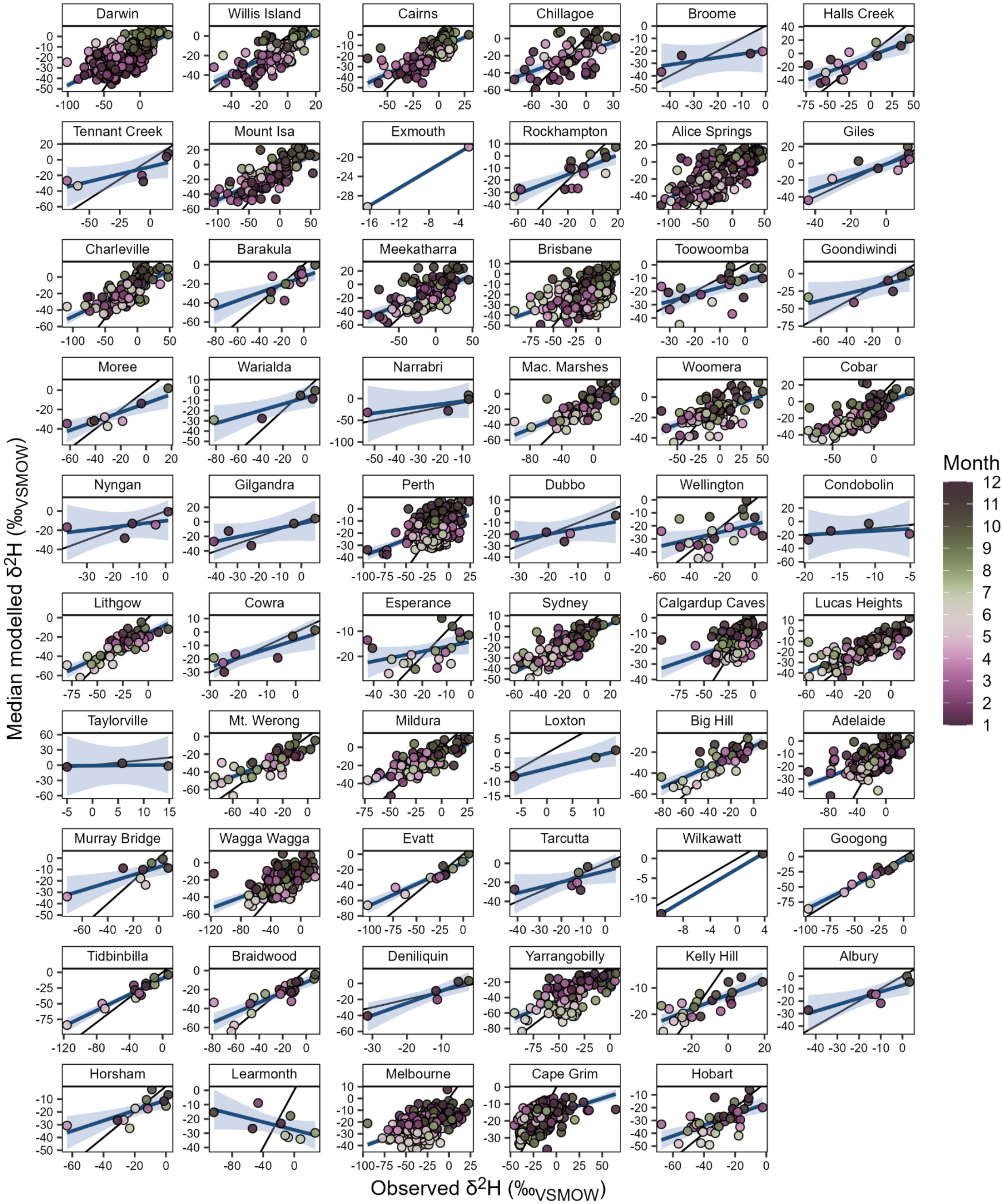

Figure S9: As per Fig. 5 but comparing modelled and observed monthly δ^2H_P values.

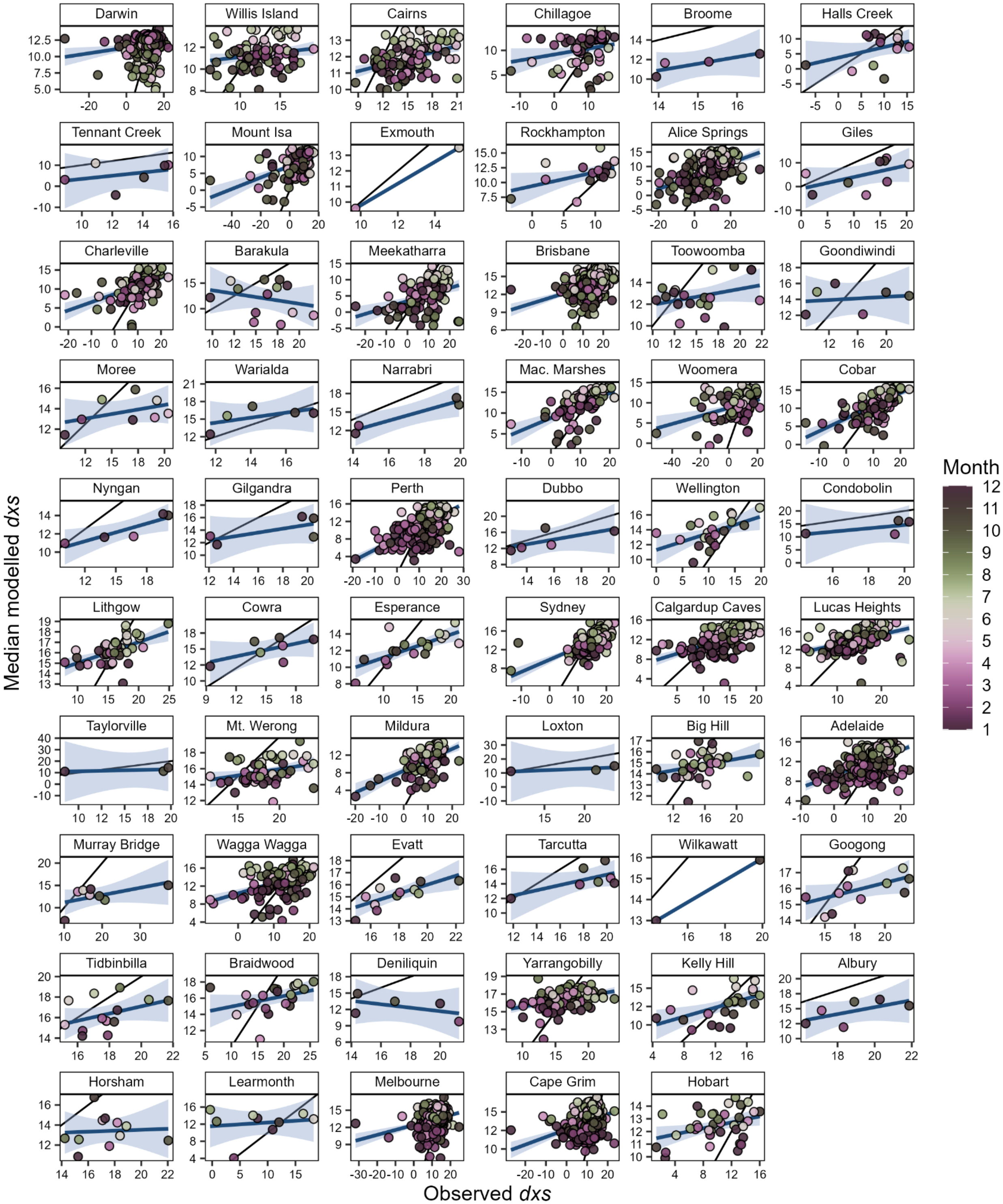

Figure S10: As per Fig. 5 but comparing modelled and observed monthly dxs_P values.

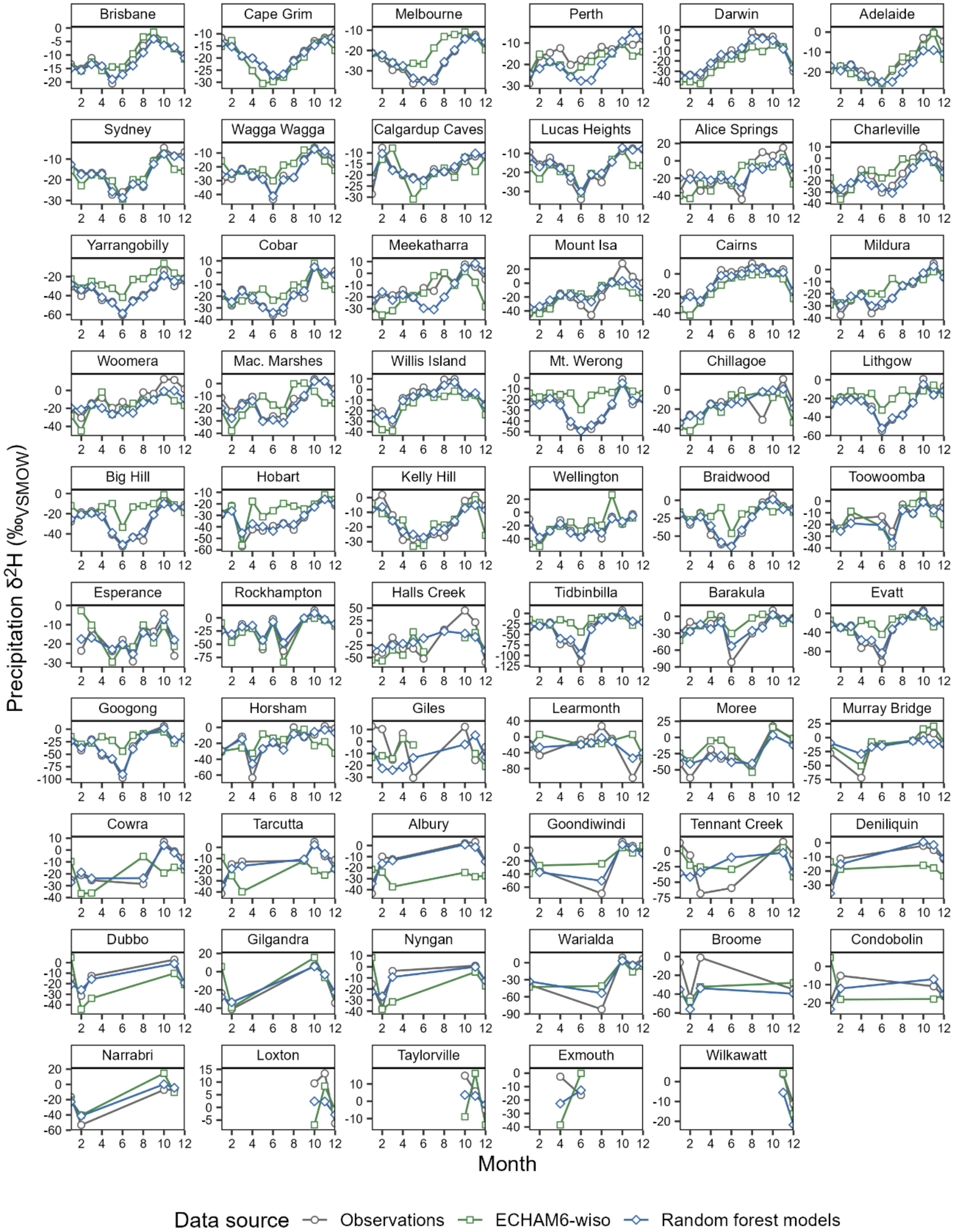

Figure S11: As per Fig. 6 but for the seasonal cycle of δ^2H_P.

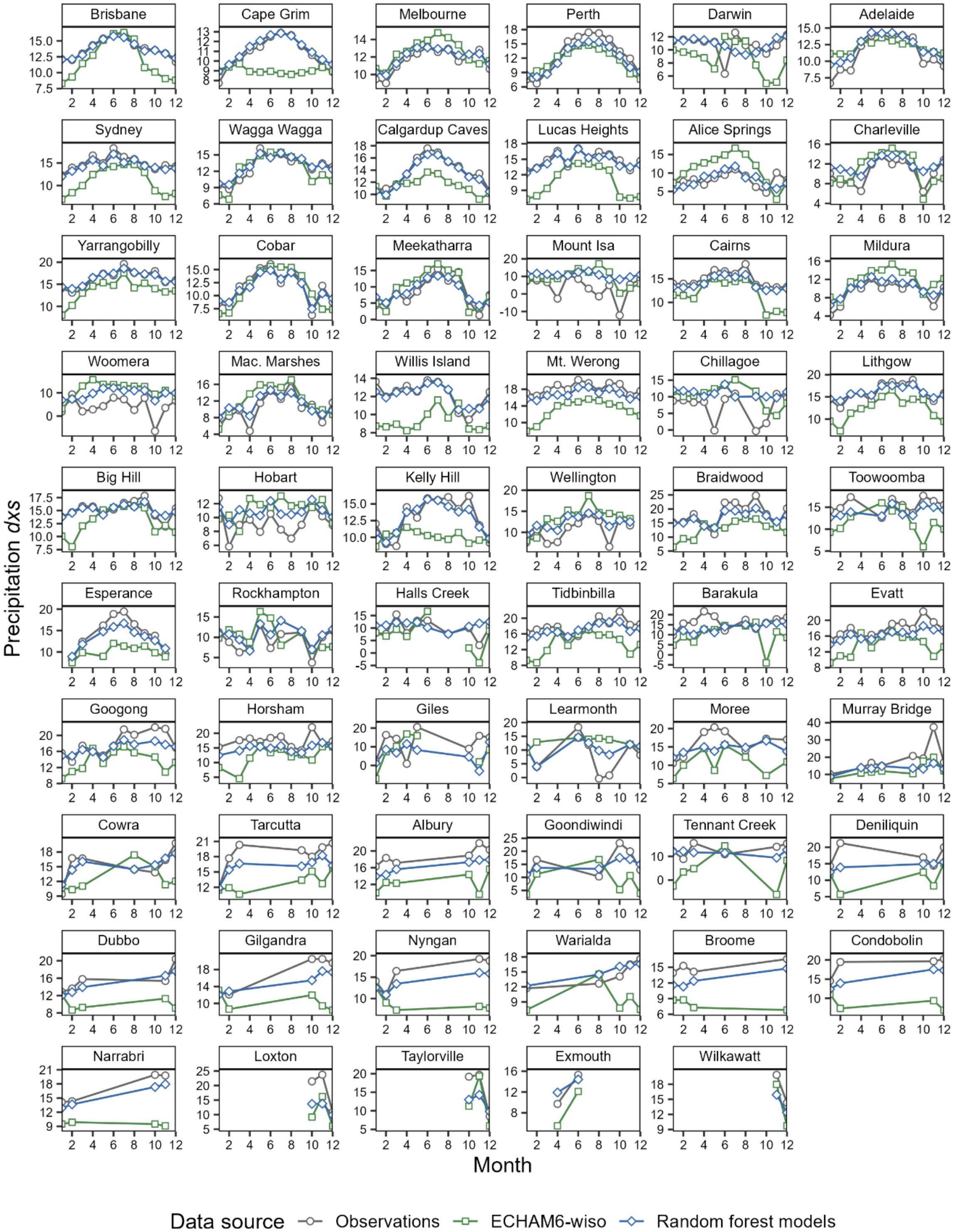

Figure S12: As per Fig. 6 but for the seasonal cycle of dxs_P.

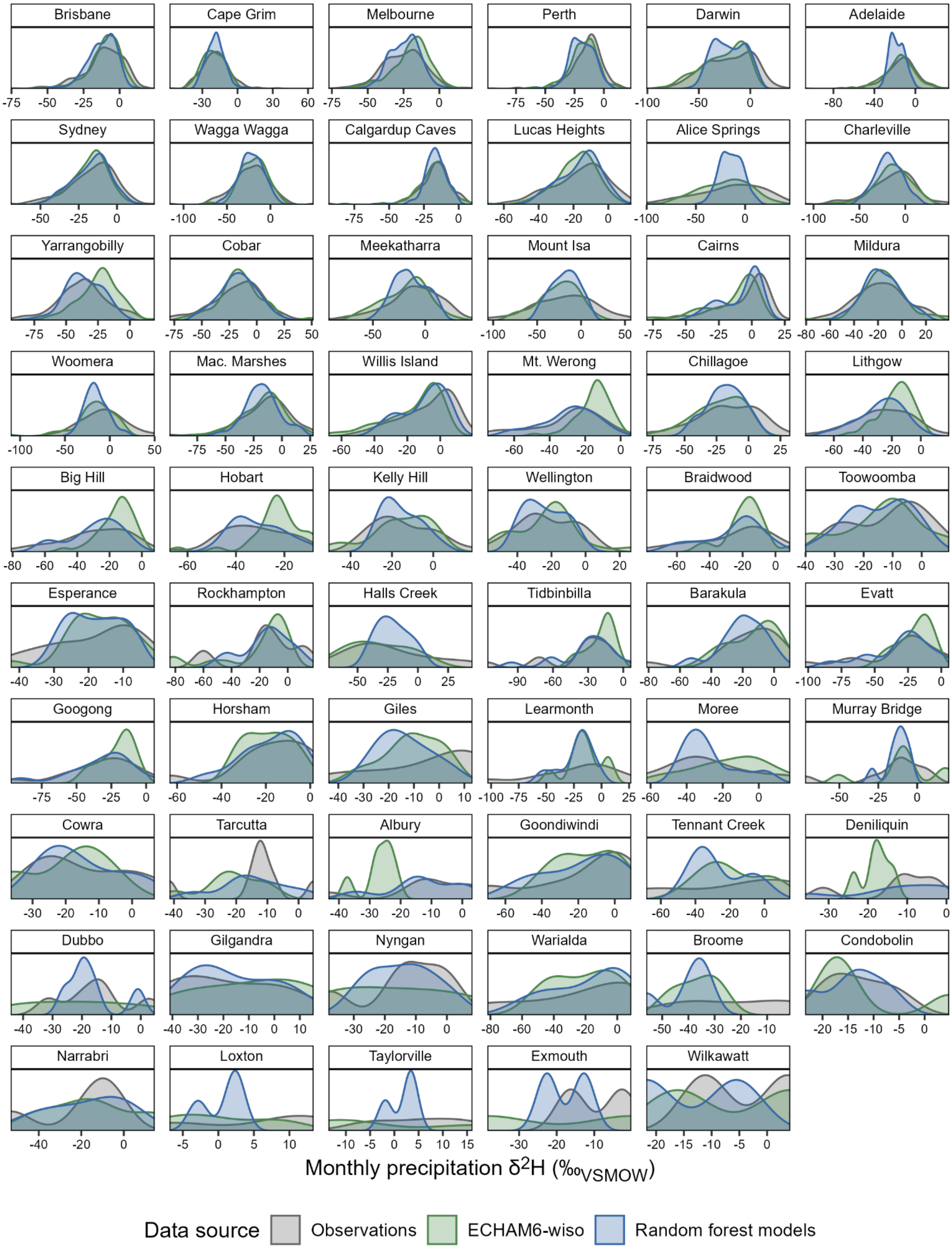

Figure S13: As per Fig. 7 but for the distribution of δ^2H_P values.

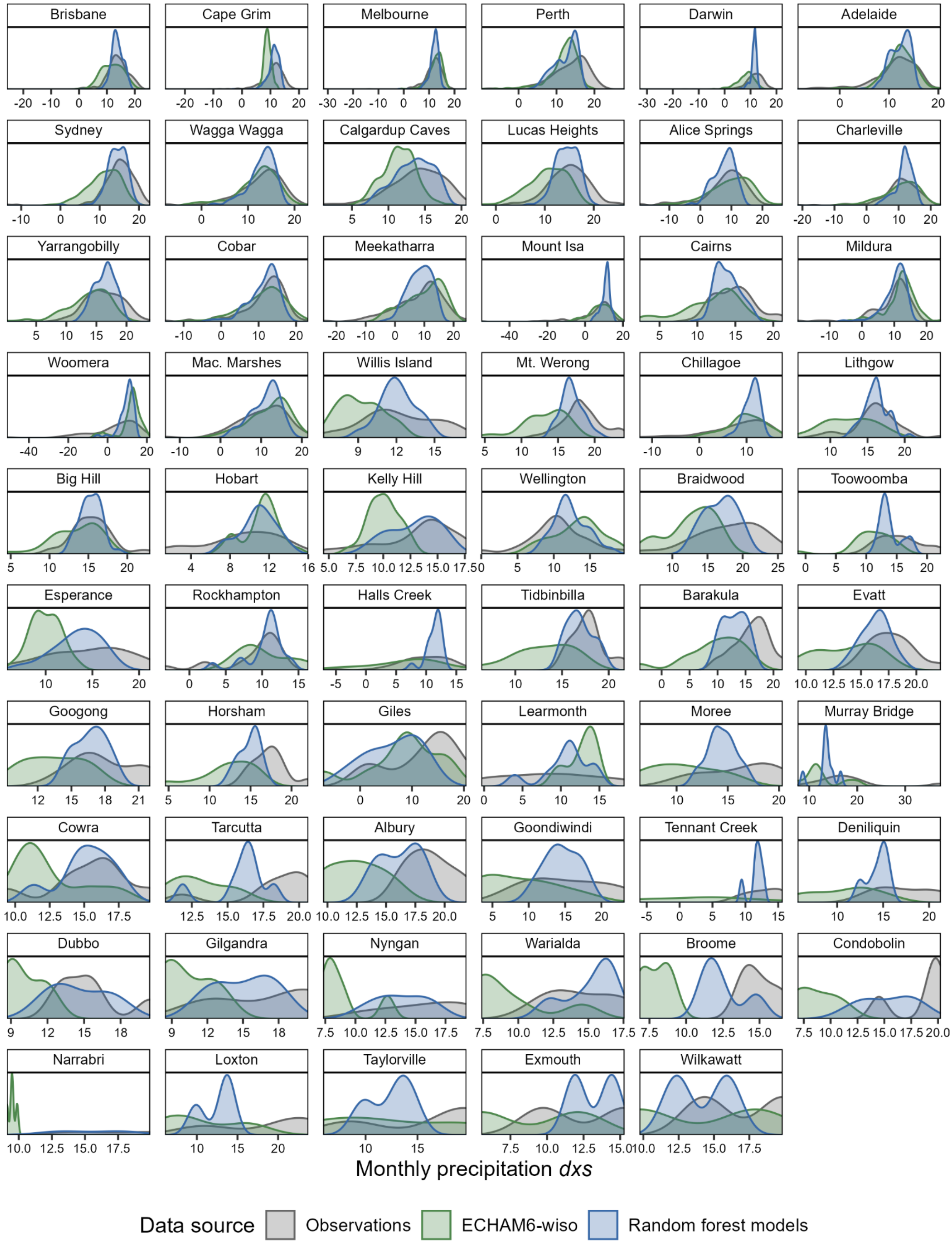

Figure S14: As per Fig. 7 but for the distribution of dxs_P values.

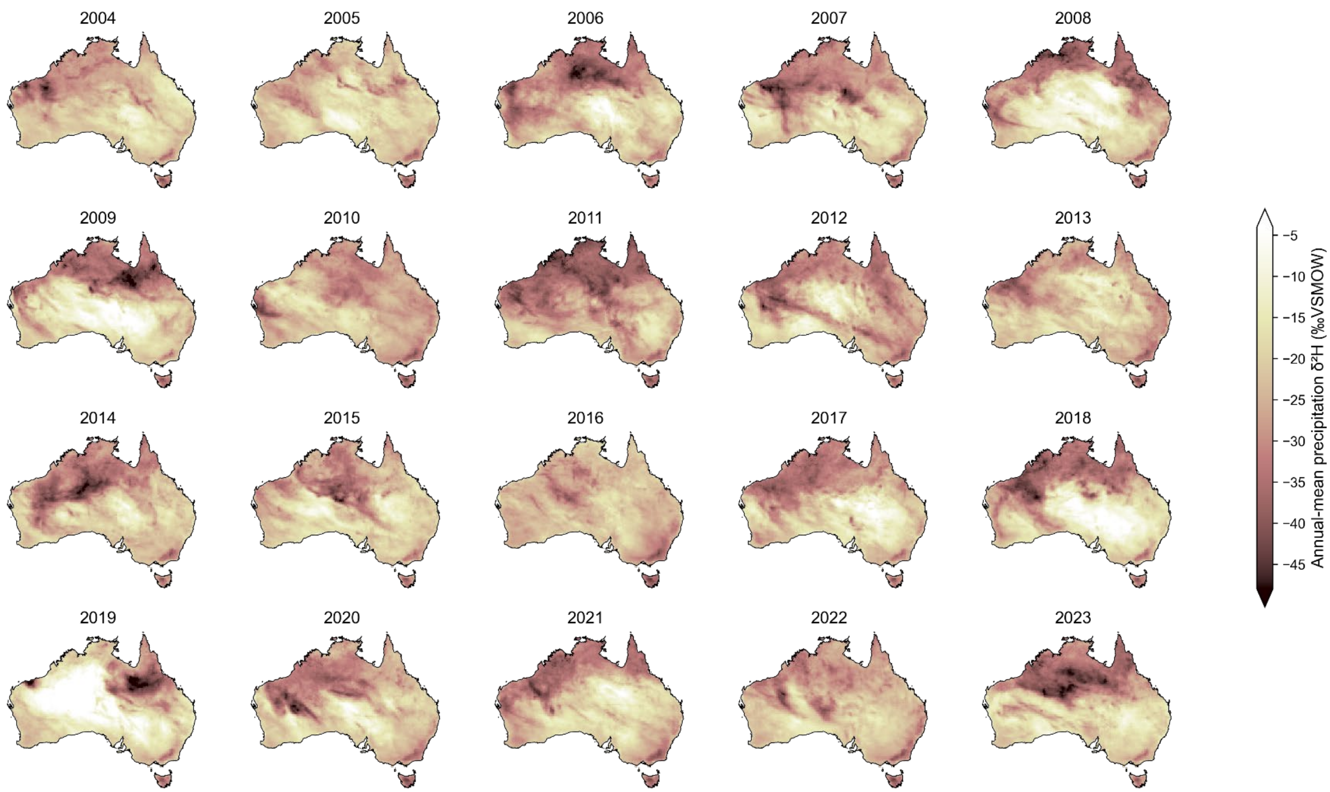

Figure S15: As per Fig. 11 but showing precipitation amount-weighted annual mean δ^2H_P values.

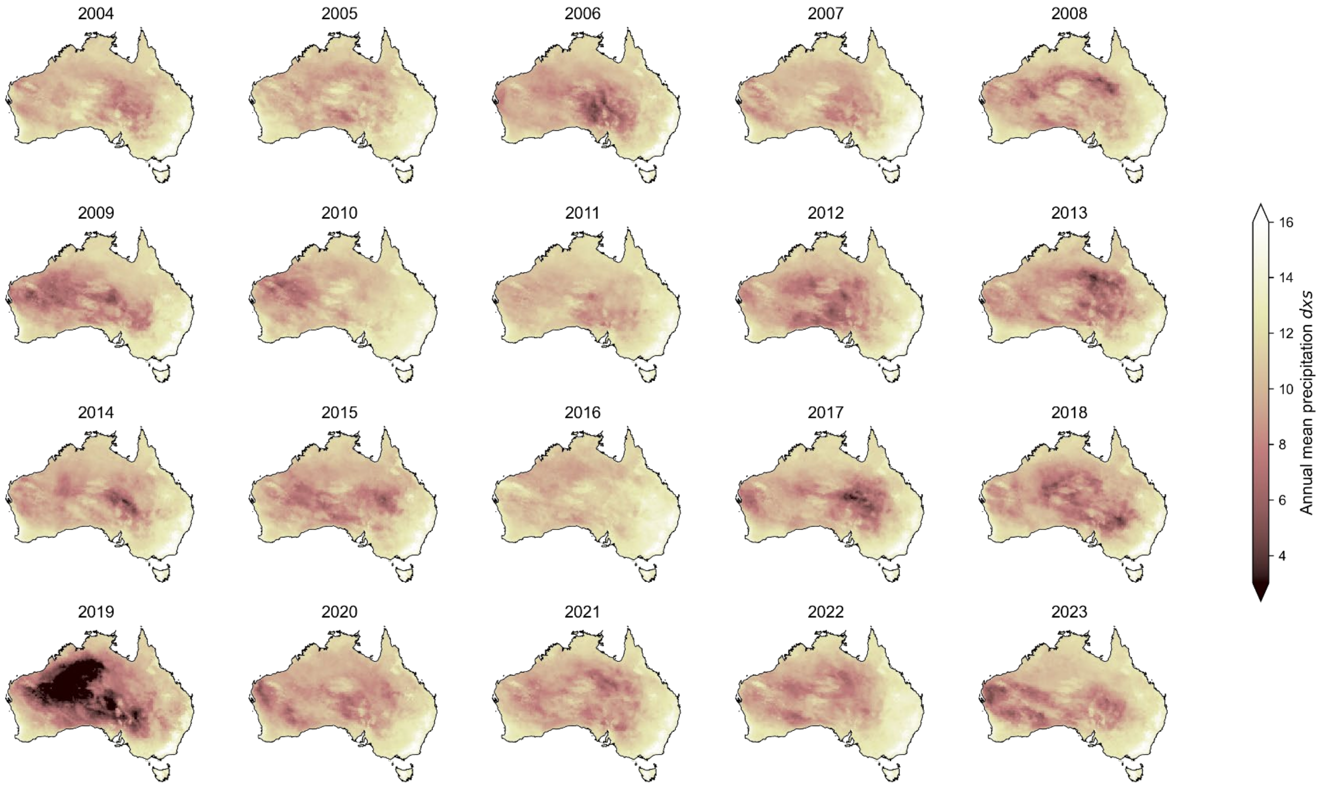

Figure S16: As per Fig. 11 but showing precipitation amount-weighted annual mean dxs_P values.

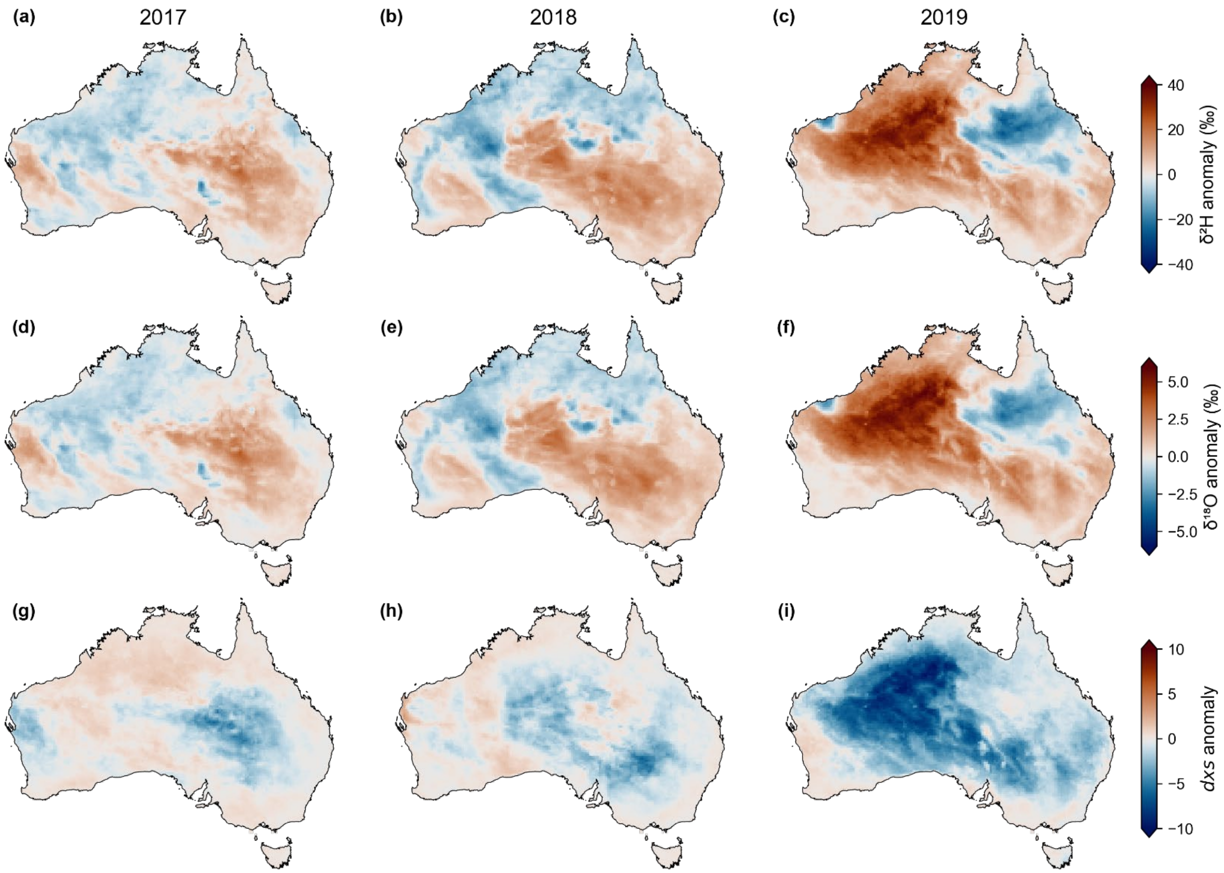

Figure S17: Anomalies in precipitation amount-weighted annual mean δ^2H_P (a–c), $\delta^{18}O_P$ (d–f) and dxs_P (g–i) in each of the three years of the Tinderbox Drought. Values are from the random forest models trained over 1962–2023, using the reduced set of predictor variables (without weather objects). Anomalies are relative to the entire 1962–2023 interval.

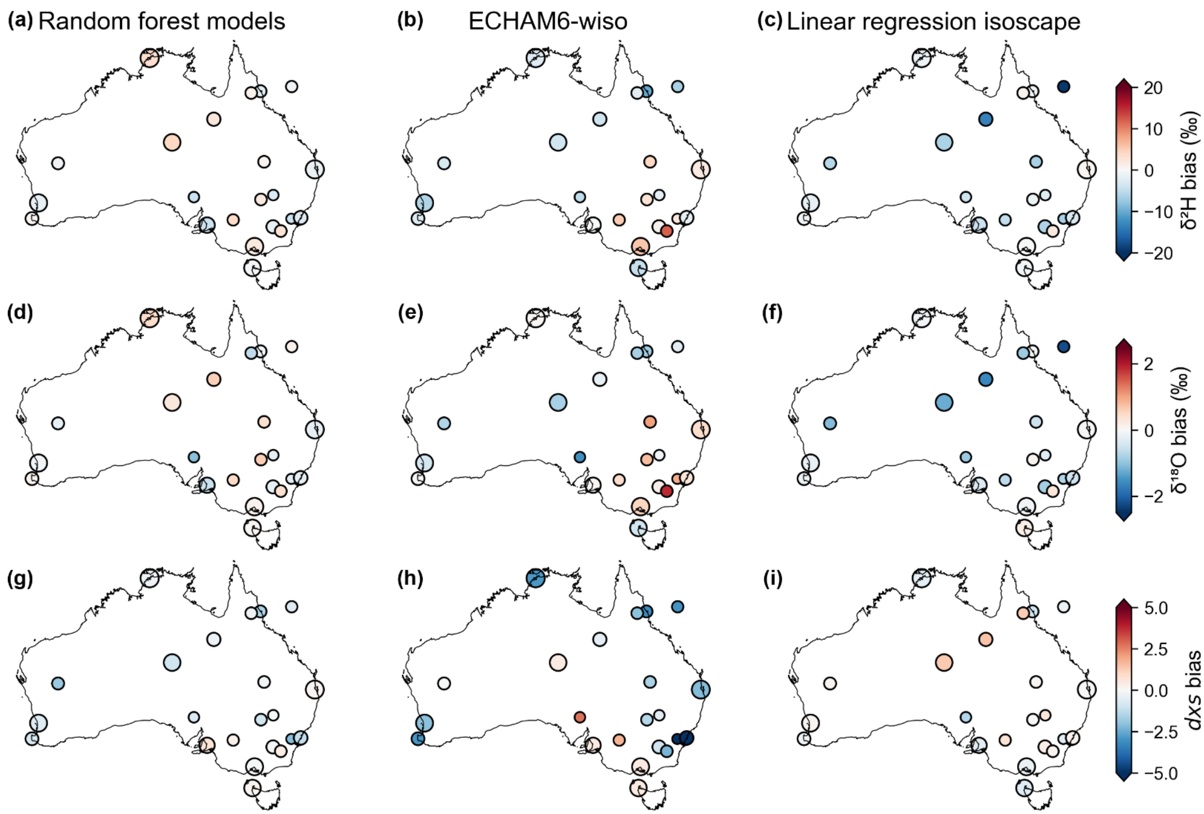

Figure S18: As per the first, second, and fourth columns of Fig. 13 but at each site showing the model's bias relative to observations in the long-term annual mean δ^2H_P (a–c), $\delta^{18}O_P$ (d–f) and dxs_P (g–h) at each site. Only showing sites with 5 or more years of monthly precipitation isotopic observations. The first column shows bias in the random forest models described in this paper (showing the mean of the 50 models created with unique random seeds); second column shows bias in ECHAM6-wiso nudged to ERA5; third column shows bias in the linear regression using geographical variables. Point size scales log-linearly with record length (in years).

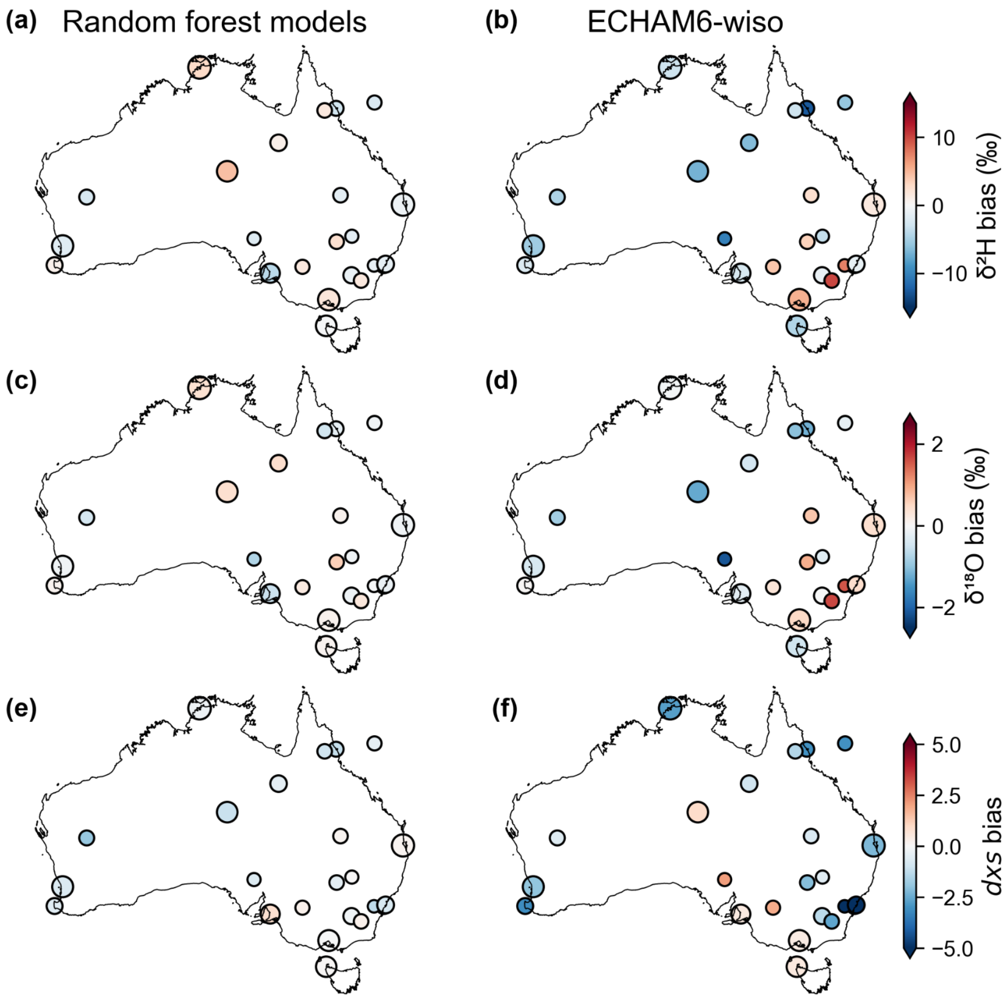

Figure S19: As per Fig. S18 but showing model bias relative to long-term observed annual means only in years included in both models (i.e., allowing direct comparison of the bias magnitudes). Note that the colour scales differ from Fig. S18.

References

Crawford, J., Hollins, S. E., Meredith, K. T., and Hughes, C. E.: Precipitation stable isotope variability and subcloud evaporation processes in a semi-arid region, Hydrol. Process., 31, 20–34, 2017.

Crawford, J., Hughes, C. E., and Chambers, S. D.: Controls on the stable isotope composition of daily precipitation in Sydney Australia: 9 years of daily data, including Radon-222, J. Hydrol. (Amst.), 617, 129123, 2023.

Crosbie, R., Morrow, D., Cresswell, R., Leaney, F., Lamontagne, S., and Lefournour, M.: New insights to the chemical and isotopic composition of rainfall across Australia, Water for a Healthy Country Flagship, CSIRO, Glen Osmond, https://doi.org/10.5072/83/5849A0D6C685A, 2012.

Cuthbert, M. O., Baker, A., Jex, C. N., Graham, P. W., Treble, P. C., Andersen, M. S., and Ian Acworth, R.: Drip water isotopes in semi-arid karst: Implications for speleothem paleoclimatology, Earth Planet. Sci. Lett., 395, 194–204, 2014.

Duvert, C., Hutley, L. B., Birkel, C., Rudge, M., Munksgaard, N. C., Wynn, J. G., Setterfield, S. A., Cendón, D. I., and Bird, M. I.: Seasonal shift from biogenic to geogenic fluvial carbon caused by changing water sources in the wet-dry tropics, J. Geophys. Res. Biogeosci., 125, https://doi.org/10.1029/2019jg005384, 2020.

Griffiths, A. D., Treble, P. C., Hope, P., and Rudeva, I.: Rainfall stable water isotope variability in coastal southwestern western Australia and its relationship to climate on multiple timescales, J. Geophys. Res., 127, https://doi.org/10.1029/2021jd035433, 2022.

Hawkins, S., Northey, J., Schroder, I., Lem, A., Sedgmen, A., and Peljo, M.: Hydrochemistry database (HYDROCHEM), https://doi.org/10.26186/147298, 2022.

Hollins, S. E., Hughes, C. E., Crawford, J., Cendón, D. I., and Meredith, K. T.: Rainfall isotope variations over the Australian continent--implications for hydrology and isoscape applications, Sci. Total Environ., 645, 630–645, 2018.

Hughes, C. E. and Crawford, J.: Spatial and temporal variation in precipitation isotopes in the Sydney Basin, Australia, J. Hydrol., 489, 42–55, 2013.

Hughes, C. E., Hegarty, N. R., Farrawell, K.-A. L., and Chisari, R.: Australian rainfall $\delta^{18}O$ and $\delta^{2}H$ data 2015-2024 (GNIP) (1.0) [Data set]. https://doi.org/10.5281/zenodo.17773309, 2025.

Jin, C., Reeder, M. J., Gallant, A. J. E., Parker, T., and Sprenger, M.: Changes in weather systems during anomalously wet and dry years in southeastern Australia, J. Clim., 37, 1131–1153, 2024.

Munksgaard, N. C., Kurita, N., Sánchez-Murillo, R., Ahmed, N., Araguas, L., Balachew, D. L., Bird, M. I., Chakraborty, S., Kien Chinh, N., Cobb, K. M., Ellis, S. A., Esquivel-Hernández, G., Ganyaglo, S. Y., Gao, J., Gastmans, D., Kaseke, K. F., Kebede, S., Morales, M. R., Mueller, M., Poh, S. C., Santos, V. D., Shaoneng, H., Wang, L., Yacobaccio, H., and Zwart, C.: Data Descriptor: Daily observations of stable isotope ratios of rainfall in the tropics, Sci. Rep., 9, 14419, 2019.

Munksgaard, N. C., Zwart, C., Haig, J., Cernusak, L. A., and Bird, M. I.: Coupled rainfall and water vapour stable isotope time series reveal tropical atmospheric processes on multiple timescales, Hydrol. Process., 34, 111–124, 2020.

Saji, N. H., Goswami, B. N., Vinayachandran, P. N., and Yamagata, T.: A dipole mode in the tropical Indian Ocean, Nature, 401, 360–363, 1999.

Sonntag, D.: Important new values of the physical constants of 1986, vapour pressure formulations based on ITS-90 and psychrometer formulae, Zeitschrift fur Meteorologie, 40, 340–344, 1990.

Vecchi, G. A., Soden, B. J., Wittenberg, A. T., Held, I. M., Leetmaa, A., and Harrison, M. J.: Weakening of tropical Pacific atmospheric circulation due to anthropogenic forcing, Nature, 441, 73–76, 2006.

Velasquez-Jimenez, L. and Abram, N. J.: Technical note: An improved methodology for calculating the Southern Annular Mode index to aid consistency between climate studies, Clim. Past, 20, 1125–1139, 2024.

Yu, L., Zhong, S., Vihma, T., Sui, C., and Sun, B.: The impact of the Indian ocean basin mode on antarctic sea ice concentration in interannual time scales, Geophys. Res. Lett., 49, https://doi.org/10.1029/2022gl097745, 2022.

Zwart, C., Munksgaard, N. C., Protat, A., Kurita, N., Lambrinidis, D., and Bird, M. I.: The isotopic signature of monsoon conditions, cloud modes, and rainfall type, Hydrol. Process., 32, 2296–2303, 2018.